Substituent Effects on Electrophilic Catalysis by the Carbonyl Group: Anatomy of the Rate Acceleration for PLP-Catalyzed Deprotonation of Glycine

Juan Crugeiras,[†] Ana Rios,*[,†] Enrique Riveiros,[†] and John P. Richard*[,‡]

[†]Departamento de Química Física, Facultad de Química, Universidad de Santiago, 15782 Santiago de Compostela, Spain
[‡]Department of Chemistry, University at Buffalo, SUNY, Buffalo, New York 14260, United States

Ⓢ *Supporting Information*

ABSTRACT: First-order rate constants, determined by ^{1}H NMR, are reported for deuterium exchange between solvent D_2O and the α-amino carbon of glycine in the presence of increasing concentrations of carbonyl compounds (acetone, benzaldehyde, and salicylaldehyde) and at different pD and buffer concentrations. These rate data were combined with ^{1}H NMR data that define the position of the equilibrium for formation of imines/iminium ions from addition of glycine to the respective carbonyl compounds, to give second-order rate constants

k_{DO} for deprotonation of α-imino carbon by DO^-. The assumption that these second-order rate constants lie on linear structure—reactivity correlations between log k_{OL} and pK_a was made in estimating the following pK_a's for deprotonation of α-imino carbon: $pK_a = 22$, glycine—acetone iminium ion; $pK_a = 27$, glycine—benzaldehyde imine; $pK_a \approx 23$, glycine—benzaldehyde iminium ion; and, $pK_a = 25$, glycine—salicylaldehyde iminium ion. The much lower pK_a of 17 [Toth, K.; Richard, J. P. *J. Am. Chem. Soc.* **2007**, *129*, 3013−3021] for carbon deprotonation of the adduct between 5′-deoxypyridoxal (**DPL**) and glycine shows that the strongly electron-withdrawing pyridinium ion is unique in *driving* the extended delocalization of negative charge from the α-iminium to the α-pyridinium carbon. This favors carbanion protonation at the α-pyridinium carbon, and catalysis of the 1,3-aza-allylic isomerization reaction that is a step in enzyme-catalyzed transamination reactions. An analysis of the effect of incremental changes in structure on the activity of benzaldehyde in catalysis of deprotonation of glycine shows the carbonyl group electrophile, the 2-O$^-$ ring substituent and the cation pyridinium nitrogen of **DPL** each make a significant contribution to the catalytic activity of this cofactor analogue. The extraordinary activity of **DPL** in catalysis of deprotonation of α-amino carbon results from the summation of these three smaller effects.
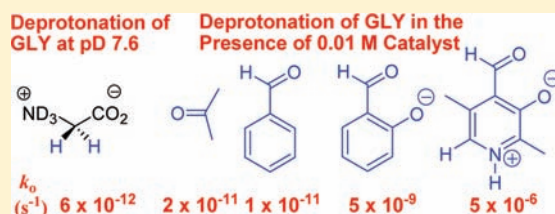
1. INTRODUCTION

We have worked over the last 15 years to characterize kinetic and thermodynamic barriers for deprotonation of the α-amino carbon of amino acids[1,2] (Chart 1) and peptides[3] in water and to understand the mechanism by which enzymes lower these barriers in catalysis of deprotonation of amino acids.[2,4] Natural selection of small molecule catalysts has seen the evolution of pyridoxal 5′-phosphate as a cofactor for an enormous range of enzymes[5−9] that catalyze deprotonation of α-amino acid carbon as the first step of more complex reactions. These enzymatic reactions include, racemization[10−12] and decarboxylation[13−18] of the amino acid, transamination to form an α-keto acid and pyridoxamine 5′-phosphate,[19−22] replacement of good nucleofuges at the β-amino position through elimination of the leaving group from a pyridoxal-stabilized carbanion to form an activated alkene, which undergoes addition of a second nucleophile,[23,24] and aldol type addition of the pyridoxal stabilized glycine carbanion to formaldehyde[25] or acetaldehyde.[26]

Our earliest studies on catalysis of deprotonation of amino acids focused on determining the effect of alkylation of the amino nitrogen and the carboxylate oxygen on the carbon acidity of glycine (Chart 1).[1,2] We next examined electrophilic catalysis of deprotonation of glycine methyl ester by the simple ketone acetone (**1**, Chart 1)[27,28] and of glycine by the pyruvoyl analogue phenylglyoxylate (**PG**)[28] through the corresponding α-iminium ion reaction intermediates (e.g., **1-IMH**). Finally, we have examined catalysis of deprotonation of glycine by 5′-deoxypyridoxal (**DPL**, Chart 2) over a broad range of pH.[29]

The effective catalysis of deprotonation of the α-amino carbon of glycine by acetone[28] shows that the carbonyl group of **PLP** is the underlying source of the catalytic power of **PLP**. This carbonyl group catalysis is assisted by other functionality at the cofactor. Most importantly, by the pyridinium nitrogen and the 2-O$^-$ substituent at the pyridine ring. There has been speculation about the role of these substituents in catalysis of deprotonation of α-amino carbon,[30] but these roles have not been rigorously evaluated. An understanding of these substituent effects will provide assistance to the development of effective small molecule

catalysts of these reactions,[31] and insight into the mechanism of action of enzymes that utilize **PLP** as a cofactor.[9]

The 5′-phosphate of **PLP** should not strongly activate the cofactor for deprotonation of α-amino acids. The most likely role for this functional group is to provide binding energy for stabilization of the Michaelis complex and the transition states for reactions in which **PLP** serves as a cofactor.[32−34] The α-amino acid carbanion should be stabilized by delocalization of negative charge onto the pyridinium nitrogen of **DPL-IMH₂**, compared to delocalization onto the neutral pyridine nitrogen of **DPL-IMH** or onto the phenyl ring of **3-IMH**. However, the amino acid carbanion is already highly delocalized at **3-IMH**, and this should cause an attenuation of the effect of the cationic nitrogen at the 4-position of the pyridine ring on the stability of the carbanion.[35] We report here the results of experiments that allow a comparison of the activities of **DPL** and salicylaldehyde (**3**) as catalysts of deprotonation of glycine.

The 2-O⁻ substituent at **DPL** and salicylaldehyde activates aldehydes for catalysis by stabilization of the iminium ion glycine adducts **DPL-IMH₂** and **3-IMH** by an intramolecular hydrogen bond to the iminium nitrogen.[36] This effect is probably attenuated, because partial proton transfer from the cationic nitrogen to oxygen will cause the charge at this nitrogen and the resulting electrostatic stabilization of the α-amino acid carbanion to decrease. We report here the results of a study of deprotonation of glycine catalyzed by **2** and by **3** that defines the contribution of this 2-O⁻ substituent to catalysis of deprotonation of glycine by **DPL**.
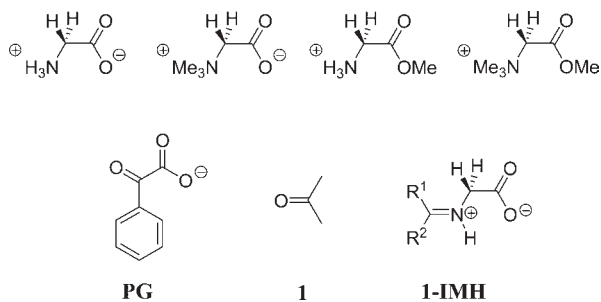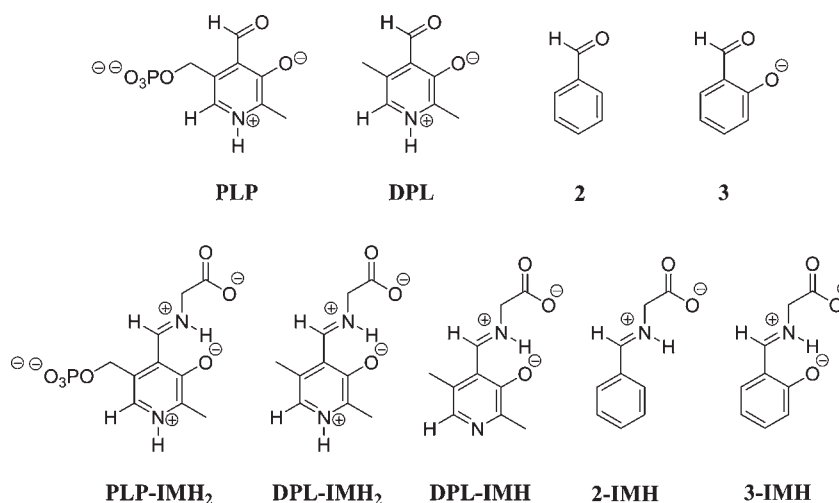
Chart 1

PG   **1**   **1-IMH**

2. EXPERIMENTAL SECTION

2.1. Materials. Glycine and salicylaldehyde were purchased from Fluka. Benzaldehyde, 1,1,1,3,3,3-hexafluoro-2-propanol (HFIP), 2,2,2-trifluoroethanol (TFE), deuterium chloride (37 wt %, 99.5% D), potassium deuterioxide (40 wt %, 98 + % D), deuterium oxide (99.9% D), and acetone-d_6 (99.9 atom % D) were from Aldrich. All other organic and inorganic chemicals were reagent grade and were used without further purification.

2.2. General Methods. The acidic protons of glycine, K_2HPO_4, and KH_2PO_4 were exchanged for deuterium before preparation of solutions of these compounds in D_2O.[2] Salicylaldehyde, HFIP, and TFE were dissolved directly in D_2O, which introduced <1 atom % of protium into this solvent. Phosphate buffers were prepared by mixing stock solutions of K_2DPO_4 and KD_2PO_4 in D_2O at $I = 1.0$ (KCl) to give the desired acid/base ratio. Pyrophosphate and carbonate buffers were prepared by dissolving a measured amount of KCl and the basic form of the buffer in D_2O, and adding DCl to give the desired acid/base ratio at $I = 1.0$ (KCl). Buffers of HFIP and TFE were prepared by dissolving a measured amount of KCl and adding KOD to give the desired acid/base ratio at $I = 1.0$ (KCl).

Solution pD was determined at 25 °C using an Orion model 350 pH meter equipped with a radiometer pHC4006-9 electrode. Values of pD were obtained by adding 0.4 to the observed reading of the pH meter.[37] The concentration of deuterioxide ion at any pD was calculated using eq 1, where $K_w = 10^{-14.87}$ is the ion product of deuterium oxide at 25 °C and $\gamma_{OL} = 0.78$ is the apparent activity coefficient of lyoxide ion under our experimental conditions.[38]

$$[DO^-] = \frac{10^{pD - pK_w}}{\gamma_{OL}} \quad (1)$$

2.3. ¹H NMR Analyses. ¹H NMR spectra at 500 MHz were recorded in D_2O at 25 °C on a Bruker AMX500 NMR spectrometer as described previously.[38,39] In all cases, the relaxation delay between pulses was at least 10-fold greater than the longest relaxation time of the protons of interest. Spectra were obtained with a sweep width of 2600 Hz, a 90° pulse angle and an acquisition time of 6 s. Baselines were corrected for drift before integration of the peaks. Chemical shifts are reported relative to $(CH_3)_4N^+$ at 2.94 ppm.

2.4. Determination of Equilibrium Constants. The position of the equilibrium for addition of glycine to acetone to form the corresponding imine in D_2O at 25 °C and $I = 1.0$ (KCl) was determined by ¹H NMR spectroscopy as described in previous work.[28,36] Formation of the imine was monitored in solutions that contained 0.1 M glycine and

Chart 2

PLP   **DPL**   **2**   **3**

PLP-IMH₂   **DPL-IMH₂**   **DPL-IMH**   **2-IMH**   **3-IMH**

1.0 M acetone at $I = 1.0$ (KCl). The pD was maintained by use of 0.10 M of the following buffers: phosphate, pD 6.1−8.0; pyrophosphate, pD 8.6−9.5; carbonate, pD 10.0−11.1; and TFE, pD 12.0−13.0.

Values of the observed equilibrium constant $(K_{add})_{obsd}$ (M^{-1}) for imine formation were determined from the ratio of the integrated areas of the peaks for the methylene protons of the imine product $(A_{CH_2}^{1-IM})$, and of the reactant glycine $(A_{CH_2}^{Gly})$ according to eq 2, where $[1-IM]_e$ and $[Gly]_e$ are the total equilibrium concentrations of imine and glycine, respectively. The ratio of equilibrium concentrations of imine adduct and amino acid was determined 1−2 h after mixing the reactants except at pD > 8, where it was determined after 24 h in order to ensure that chemical equilibrium had been reached. Acetone-catalyzed deuterium incorporation into glycine also took place during this time period at pD 13. However, ^{1}H NMR analysis showed the same deuterium enrichment of the α-CH$_2$ groups of glycine and of the imine within experimental error. Therefore, the ratio of the equilibrium concentrations of imine adduct and glycine was determined as the ratio of the sum of peak areas for the −CH$_2$− and −CHD− groups.

$$(K_{add})_{obsd} = \frac{[1-IM]_e}{[Gly]_e[Acetone]} = \frac{A_{CH_2}^{1-IM}}{A_{CH_2}^{Gly}[Acetone]} \qquad (2)$$

2.5. Kinetic Measurements.

All reactions were carried out in D$_2$O at 25 °C and $I = 1.0$ (KCl). The deuterium-exchange reactions of glycine in the presence of acetone or **3** were initiated by mixing solutions of glycine, the catalyst, and the buffer at the same pD and ionic strength $(I = 1.0$ (KCl)). The final concentration of the amino acid ranged from 5 to 15 mM. The deuterium exchange reactions of glycine in the presence of **2**, in alkaline solutions of D$_2$O, were initiated by mixing solutions of glycine, **2**, and KOD at the same ionic strength $(I = 1.0$ (KCl)) to give a final glycine concentration of 5 mM.

The exchange for deuterium of the first α-proton of glycine was followed by monitoring the disappearance of the singlet due to the α-CH$_2$ group of the substrate and the appearance of the upfield-shifted triplet due to the α-CHD group of the monodeuterated product by ^{1}H NMR spectroscopy at 500 MHz, as described in previous work.[2,27,28] Values of R, which is a measure of the progress of the deuterium-exchange reaction, were calculated using eq 3, where A_{CH_2} and A_{CHD} are the integrated areas of the peaks for the α-CH$_2$ and the α-CHD groups, respectively. The reactions in the presence of acetone, **2** and **3** were followed during exchange for deuterium of 20−30%, 40−90%, and 60−90%, respectively, of the first proton of the α-CH$_2$ group of the substrate. In all cases an equilibrium mixture of glycine and the corresponding imine was observed before the formation of a significant amount of deuterium-labeled glycine. Semilogarithmic plots of reaction progress, R, against time according to eq 4 were linear with negative slopes equal to k_{obsd} (s^{-1}), which is the rate constant for exchange of a *single* proton of the α-CH$_2$ group of the substrate. The values of the first-order rate constant for exchange of the first α-CH$_2$ proton to give the monodeuterated product, k_{ex} (s^{-1}), were determined as $k_{ex} = 2\,k_{obsd}$.

$$R = \frac{A_{CH_2}}{A_{CH_2} + A_{CHD}} \qquad (3)$$

$$\ln R = -k_{obsd}t \qquad (4)$$

3. RESULTS

3.1. Equilibrium Constants for Imine Formation.

Figure 1 shows the change with changing pD in the observed chemical shift $(\delta_{CH_2})_{obsd}^{1-IM}$ (ppm) of the signal for the α-CH$_2$ hydrogens of the mixture of **1-IM** and **1-IM-D** (Scheme 1) which forms in D$_2$O from the reaction of 0.1 M glycine and 1.0 M acetone at 25 °C and $I = 1.0$ (KCl). The change in the chemical shift of
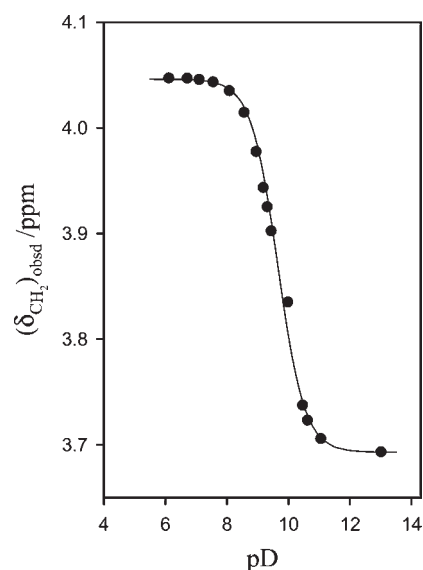

Figure 1. The dependence on pD of $(\delta_{CH_2})_{obsd}$ (ppm) for the −CH$_2$− hydrogen of the imine formed in D$_2$O that contains 0.1 M glycine and 1 M acetone at 25 °C and $I = 1.0$ (KCl). The solid line shows the fit of the data to eq 5 derived for Scheme 1.

the α-methylene group is due to the change in the protonation state of the imine nitrogen. The solid line in Figure 1 shows the nonlinear least-squares fit of the data to eq 5, derived for Scheme 1, where (a) $\delta_{CH_2}^{1-IM-D} = 4.05$ ppm and $\delta_{CH_2}^{1-IM} = 3.69$ ppm are the chemical shifts for the α-CH$_2$ group observed at limiting low and high pD, and (b) the value of $(K_a)_{1-IM-D} = 10^{-9.64}$ is determined by treating this acidity constant as a variable parameter.

$$(\delta_{CH_2})_{obsd}^{1-IM} = \frac{\delta_{CH_2}^{1-IM}(K_a)_{1-IM-D} + \delta_{CH_2}^{1-IM-D} a_D}{((K_a)_{1-IM-D} + a_D)} \qquad (5)$$

Values of the apparent equilibrium constants $(K_{add})_{obsd}$ (M^{-1}) for addition of glycine to acetone to form the corresponding imine in D$_2$O at 25 °C were determined by ^{1}H NMR analysis, as described in the Experimental Section. Figure 2 shows the change, with changing pD, in log $(K_{add})_{obsd}$ for addition of glycine to acetone. The line shows the fit of the data to eq 6, derived for Scheme 1, using $(K_a)_{GlyD} = 3.5 \times 10^{-11}$ M, $(K_a)_{1-IM-D} = 2.3 \times 10^{-10}$ M (Table 1) and $(K_{add})_{1-IM-D} = 0.0056$ M^{-1} determined for the formation of the iminium ion at pD < 8.

$$(K_{add})_{obsd} = (K_{add})_{1-IM-D} \left(\frac{a_D + (K_a)_{1-IM-D}}{a_D + (K_a)_{GlyD}} \right) \qquad (6)$$

3.2. Deuterium Exchange Reactions. 3.2.1. Catalysis by Acetone.

The exchange for deuterium of the first α-proton of glycine in D$_2$O at 25 °C and $I = 1.0$ (KCl) was monitored by ^{1}H NMR spectroscopy (500 MHz) as described previously.[2,28] Table S1 of the Supporting Information gives the observed first-order rate constants k_{ex} (s^{-1}) for deuterium exchange in the presence of various concentrations of acetone and HFIP buffer at pD 9.3, 9.9, and 10.5, determined as described in the Experimental Section. Figure 3 shows the effect of increasing concentrations of HFIP buffer (50% free base) on k_{ex} (s^{-1}) for reactions at different fixed concentrations of acetone. The intercepts of these linear correlations are the first-order rate constants $k_o = k_w f_{1-IM-D}$ (s^{-1}, Table 2) for
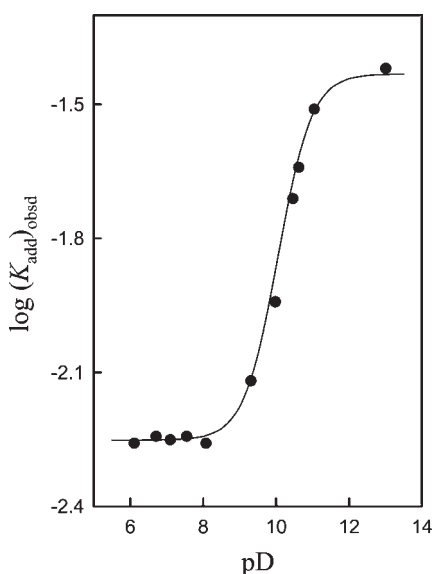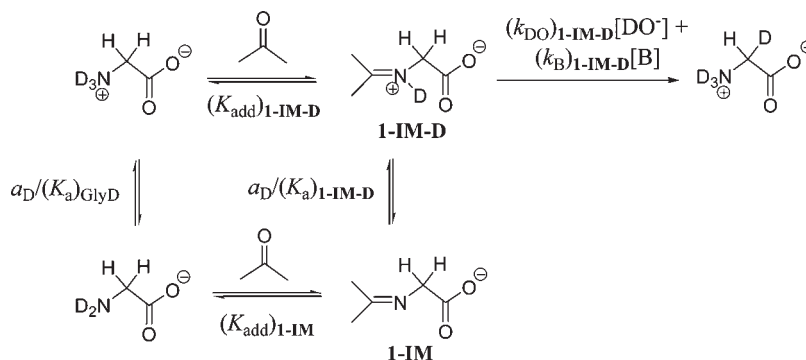
Scheme 1

Figure 2. Logarithmic dependence of $(K_{add})_{obsd}$ (M^{-1}) on pD for conversion of glycine to the acetone imine in D_2O at 25 °C and $I = 1.0$ (KCl). The solid line was calculated using eq 6 and the equilibrium constants from Table 1.

deuterium exchange catalyzed by the solvent at the given concentration of acetone, where f_{1-IM-D} is the fraction of glycine present as the iminium ion adduct **1-IM-D** (eq 7, derived for Scheme 1)[40] and k_w is the apparent first-order rate constant for the solvent reaction. Table 2 reports values of k_w, calculated as $k_w = k_o/f_{1-IM-D}$, for reactions at different concentrations of acetone.

$$f_{1-IM-D} = \frac{(K_{add})_{1-IM-D}[\text{acetone}]}{\left(1 + \frac{(K_a)_{GlyD}}{a_D}\right)} \quad (7)$$

A similar analysis of data for reactions in 20 and 80% free base HFIP buffers (Table S1) gave $k_w = 1.6 \times 10^{-5}$ s^{-1} and $k_w = 2.2 \times 10^{-4}$ s^{-1} for deprotonation of the iminium ion at pD 9.27 and 10.48, respectively. Figure 4 (▼) shows the pD-rate profile of log k_w for deprotonation of **1-IM-D** in D_2O. The solid line of unit slope shows the least-squares fit of the data to eq 8 using $(k_{DO})_{1-IM-D} = 4.2$ M^{-1} s^{-1} for deprotonation of **1-IM-D** by DO^- (Scheme 1), where $K_w = 10^{-14.87}$ M^2 is the ion product of D_2O at

Table 1. Equilibrium Constants in D_2O for Addition of Glycine to Acetone[a]

amino compound	imine	$p(K_a)_{Gly}$[b]	$p(K_a)_{X-IM-D}$[c]	K_{add}[d] (M^{-1})
$^+D_3NCH_2COO^-$	**1-IMD**	10.44 ± 0.03	9.64 ± 0.03	$(5.6 \pm 0.1) \times 10^{-3}$
$D_2NCH_2COO^-$	**1-IM**			$(3.5 \pm 0.5) \times 10^{-2}$

[a] At 25 °C and $I = 1.0$ (KCl). [b] The acidity constant of the amino acid in D_2O at 25 °C and $I = 1.0$ (KCl) determined by ^1H NMR titration. [c] Apparent acidity constant in D_2O at 25 °C and $I = 1.0$ (KCl), determined by NMR titration as described in the text. [d] Equilibrium constant for the addition of the amino acid to acetone to form the imine adduct.

25 °C and $\gamma_{OL} = 0.78$ is the apparent activity coefficient of lyoxide ion under our experimental conditions.

$$\log k_w = \log\left(\frac{k_{DO}K_w}{\gamma_{OL}}\right) + pD \quad (8)$$

The slopes of the linear correlations in Figure 3 are equal to $(k_{buf})_{obsd} = (k_B)_{1-IM-D} f_B f_{1-IM-D}$ for the deuterium exchange reaction catalyzed by buffer at the given concentration of acetone, where $(k_B)_{1-IM-D}$ $(M^{-1} s^{-1})$ is the second-order rate constant for deprotonation of **1-IM-D** by the buffer base (Scheme 1) and f_B is the fraction of the catalyst in the basic form. The values of k_B reported in Table 2 were calculated from $(k_{buf})_{obsd}$ using the appropriate values of f_B and f_{1-IM-D}. A value of $(k_B)_{1-IM-D} = 2.4 \times 10^{-4}$ M^{-1} s^{-1} for deprotonation of **1-IM-D** by the HFIP base (Scheme 1) was calculated as the average of the values of k_B determined at different fractions of buffer base.

3.2.2. Catalysis by Benzaldehyde (2). The exchange for deuterium of the first α-proton of glycine in the presence of **2** and various concentrations of deuterioxide ion in D_2O at 25 °C and $I = 1.0$ (KCl) was followed by ^1H NMR (500 MHz). Table S2 gives values of the first-order rate constant k_{ex} (s^{-1}) for the deuterium exchange reaction together with values of f_{2-IM}, the fraction of amino acid converted to the imine (Scheme 2) under the experimental reaction conditions, determined by ^1H NMR analysis of the mixture of glycine and **2** in D_2O, as described in previous work.[36] The rate constants for solvent-catalyzed deprotonation of the imine adduct, $k_w = k_{ex}/f_{2-IM}$, increase linearly with the concentration of deuterioxide ion (not shown). The slope of this correlation gives $(k_{DO})_{2-IM} = 2.90 \times 10^{-4}$ M^{-1} s^{-1} as the second-order rate constant for deprotonation of **2-IM** catalyzed

by deuterioxide ion. Figure 4 (▲) shows the pD-rate profile of log k_w for deprotonation of **2-IM** in D_2O. The solid line of unit slope shows the fit of the data to eq 8 ((k_{DO})$_{2-IM}$ = 2.90 × 10^{-4} M^{-1} s^{-1}). It was not possible to determine a value of the second-order rate constant for deprotonation of **2-IM-D** by DO$^-$ because the deuterium-exchange reaction is too slow to monitor at pD < 11, where the concentration of **2-IM-D** would begin to become significant.

3.2.3. Catalysis by Salicylaldehyde (3). The exchange for deuterium of the first α-proton of glycine was examined in D_2O at 25 °C and I = 1.0 (KCl) in solutions buffered with HFIP (pD 9.3−10.5). Table S3 of the Supporting Information gives the observed first-order rate constants k_{ex} (s^{-1}) for deuterium exchange in the presence of various concentrations of **3** and HFIP buffer at pD 9.3, 9.8 and 10.5, determined as described in the Experimental Section. Table S3 also reports values of f_{3-IM-D}, the fraction of total glycine that is converted to the reactive iminium ion adduct (Scheme 3) at each concentration of **3** at the given pD, determined by ^{1}H NMR analysis of the mixture of glycine and **3**, as described in previous work.[36] Figure 5 shows the

linear dependence of k_{ex} on the total concentration of HFIP buffer (pD 9.8) for reactions at two fixed concentrations of **3**. The intercepts of these linear plots are the first-order rate constants k_o = $k_w f_{3-IM-D}$ (s^{-1}, Table 3) for solvent-catalyzed exchange at the given pD, where k_w is the apparent first-order rate constant for the solvent reaction and f_{3-IM-D} is the fraction of glycine present as the iminium ion **3-IM-D** (Table S3). Table 3 reports values of k_w, calculated as k_w = k_o/ f_{3-IM-D}, for reactions at two different concentrations of **3**. The same treatment of the data for reactions at pD 10.5 and 9.3 (Table 3) gives k_w = 1.1 × 10^{-5} s^{-1} and k_w = 7.8 × 10^{-7} s^{-1}, respectively. The slope of a linear plot (not shown) of k_w against [DO$^-$] gives the second-order rate constant (k_{DO})$_{3-IM-D}$ = 0.19 M^{-1} s^{-1} for deprotonation of **3-IMD** by deuterioxide ion. Figure 4 (●) shows the pD-rate profile of log k_w for deprotonation of **3-IMD** in D_2O. The solid line of unit slope through the data was
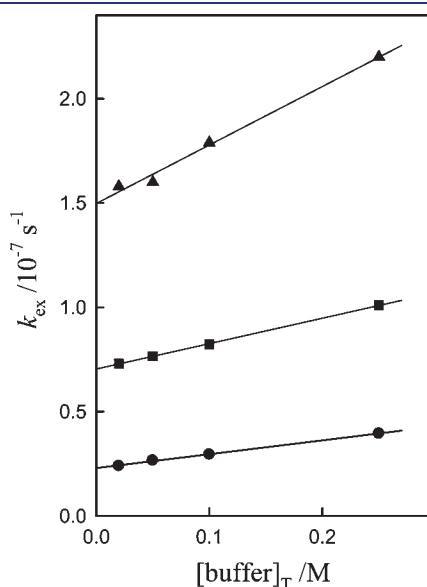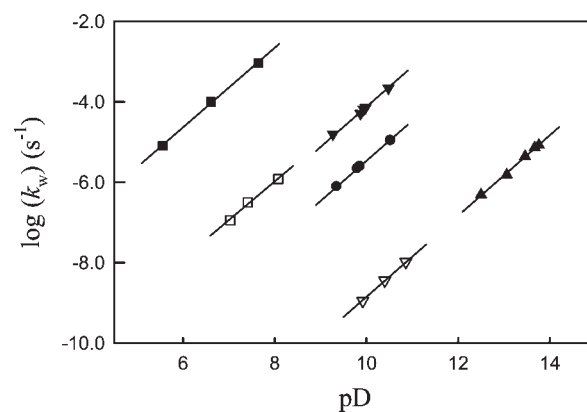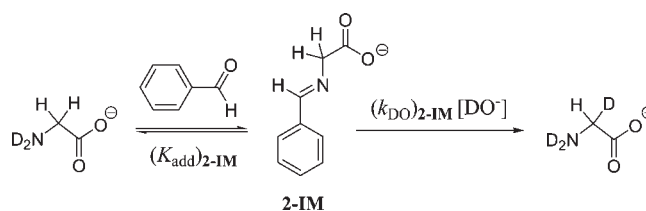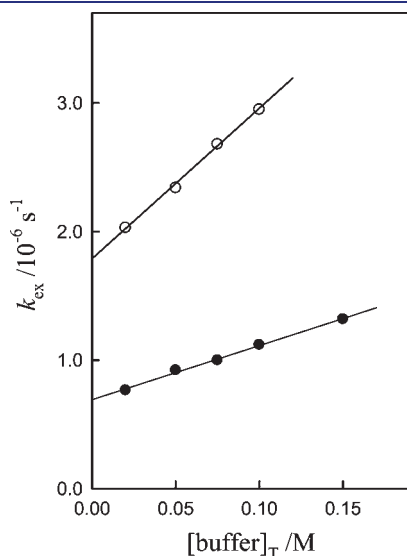
Scheme 2

2-IM

Figure 3. Dependence of k_{ex} (s^{-1}) for exchange of the first α-proton of glycine in the presence of acetone on the total concentration of HFIP buffer at pD 9.98 ([RO$^-$]/[ROH] = 1.0) in D_2O at 25 °C and I = 1.0 (KCl). Key: (●) 0.10 M acetone; (■) 0.25 M; (▲) 0.50 M.

Figure 4. pD-rate profiles of k_w (s^{-1}) for exchange for deuterium of the first α-CH$_2$ hydrogen of: (▼) **1-IM-D**; (▲) **2-IM**; (●) **3-IM-D**; (▽) N-protonated glycine;[2] (□) N-protonated glycine methyl ester;[2] (■) the acetone-glycine methyl ester iminium ion.[27,28].

Table 2. Rate Constants for Exchange of the First α-Proton of Glycine in the Presence of Acetone and HFIP Buffers in D_2O[a]

base	f_B[c]	pD	[acetone] /M	f_{1-IM-D}[d]	k_o /s^{-1e}	k_w /s^{-1f}	(k_{buf})$_{obsd}$/ M^{-1} s^{-1g}	k_B /M^{-1} s^{-1h}
HFIP	0.8	10.48	0.25	6.8 × 10^{-4}	1.5 × 10^{-7}	2.2 × 10^{-4}	1.3 × 10^{-7}	2.4 × 10^{-4}
pK_{BD} = 9.9[b]								
	0.5	9.87	0.10	4.4 × 10^{-4}	2.3 × 10^{-8}	5.1 × 10^{-5}	6.6 × 10^{-8}	3.0 × 10^{-4}
		9.94	0.25	1.1 × 10^{-3}	7.0 × 10^{-8}	6.5 × 10^{-5}	1.2 × 10^{-7}	2.3 × 10^{-4}
		9.98	0.50	2.1 × 10^{-3}	1.5 × 10^{-7}	7.1 × 10^{-5}	2.8 × 10^{-7}	2.6 × 10^{-4}
	0.2	9.27	0.25	1.3 × 10^{-3}	2.1 × 10^{-8}	1.6 × 10^{-5}	5.8 × 10^{-8}	2.2 × 10^{-4}

[a] At 25 °C and I = 1.0 (KCl). [b] Apparent pK_a of the conjugate acid in D_2O at 25 °C and I = 1.0 (KCl). [c] Fraction of the buffer present in the basic form. [d] Fraction of glycine present as the reactive iminium ion **1-IM-D**, calculated from eq 7 using the values of the equilibrium constants reported in Table 1. [e] The intercept of plots of k_{ex} against [buffer]$_T$ (Figure 3). [f] Apparent first-order rate constants for solvent-catalyzed deprotonation of **1-IM-D**, calculated from the values of k_o as described in the text. [g] The slope of plots of k_{ex} against [buffer]$_T$ (Figure 3). [h] Second-order rate constants for HFIP base-catalyzed deprotonation of **1-IM-D**, calculated from the values of (k_{buf})$_{obsd}$ as described in the text.

calculated from the value of k_{DO} using eq 8 and $(k_{DO})_{\text{3-IM-D}} = 0.19$ M^{-1} s^{-1}.

The slopes of the linear correlations in Figure 5 are apparent second-order rate constants, $(k_{\text{buf}})_{\text{obsd}} = (k_B)_{\text{3-IM-D}} f_B f_{\text{3-IM-D}}$ for the buffer-catalyzed deuterium exchange reaction at the given concentration of 3, where $(k_B)_{\text{3-IM-D}}$ $(M^{-1}$ $s^{-1})$ is the second-order rate constant for deprotonation of 3-IM-D by the buffer base and f_B is the fraction of the catalyst in the basic form. Table 3 reports values of k_B that were calculated from $(k_{\text{buf}})_{\text{obsd}}$ using the appropriate values of f_B and $f_{\text{3-IM-D}}$. A value of $(k_B)_{\text{3-IM-D}} = 2.9 \times 10^{-5}$ M^{-1} s^{-1} for deprotonation of 3-IM-D by the HFIP base

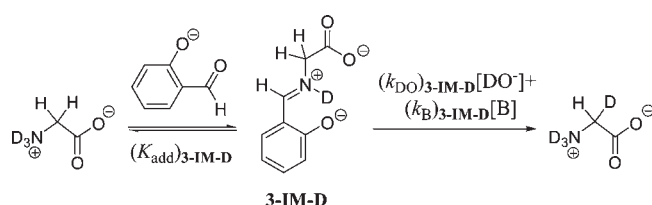**Scheme 3**

3-IM-D

Figure 5. Dependence of k_{ex} (s^{-1}) for exchange for deuterium of the first α-proton of glycine in the presence of salicylaldehyde on the total concentration of HFIP buffer at pD 9.8 in D_2O at 25 °C and $I = 1.0$ (KCl). Key: (●) 10 mM 3; (○) 52 mM 3.

was calculated as the average of the values of k_B determined at different fractions of buffer base.

4. DISCUSSION

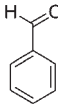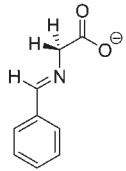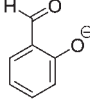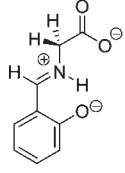Acetone (1), salicylaldehyde (3) and benzaldehyde (2) are effective catalysts of the deprotonation of the α-amino carbon of glycine in D_2O. This reaction leads to exchange of the α-hydrogen for deuterium from solvent, which is monitored by ^1H NMR. The observation that the deuterium exchange reactions are first-order in the concentration of the electrophilic catalyst and deuterioxide ion shows that they proceed by formation of imine or iminium ion adducts to glycine, which undergo deprotonation by deuterioxide ion to form enolates (Schemes 1, 2 and 3). Table 4 reports equilibrium constants K_{add} for formation of adducts between glycine and 1, 2 or 3; and, second-order rate constants k_{DO} for deprotonation of these adducts. Second-order rate constants $k_{HO} = 2.9$ M^{-1} s^{-1}, 0.13 M^{-1} s^{-1}, and 2.0×10^{-4} M^{-1} s^{-1} (Table 5) for deprotonation of 1-IMH, 3-IMH, and 2-IM, respectively, by hydroxide ion in H_2O were calculated from the experimental values of k_{DO} and an estimated secondary solvent deuterium isotope effect of $k_{DO}/k_{HO} = 1.46$.[41] Table 5 summarizes the values of k_{HO} for deprotonation of glycine and derivatives of glycine reported here and in earlier work.[2,28,29]

4.1. Carbon Acid pK_a's. Figure 6 (■) shows the linear relationship, with slope 0.44, between the statistically corrected values of log k_{HO} for deprotonation of *cationic* ketones and esters, and the pK_a of the carbon acid.[2] The carbon acid pK_a's for 1-IMH and 3-IMH reported in Table 5 were estimated by assuming that the values of log k_{OH} for these carbon acids lie on the linear correlation for other cationic ketones and esters. Figure 6 (●) also shows the linear correlation between the statistically corrected values of log k_{HO} for deprotonation of *neutral* mono-carbonyl carbon acids and the carbon acid pK_a.[38,39,42−44] A pK_a of 27 (Table 5) for the ionization of 2-IM was calculated with the assumption that the value of log k_{HO} for this carbon acid lies on this linear correlation.

The large equilibrium constant of $K_{\text{add}} = 44$ M^{-1} for formation of the Schiff base 2-IM from 2 and glycine facilitates detection of the 2-catalyzed deuterium exchange reaction of glycine at high pD (Figure 4). It was not possible to detect the 2-catalyzed deuterium exchange reaction of glycine at low pD, where 2-IMD is the reacting carbon acid, because $(K_{\text{add}})^+ = 0.0033$ M^{-1} for formation of 2-IMD is very small (Table 4), and the low solubility of benzaldehyde in water prevents experiments with concentrations of aldehyde larger than 0.02 M.

Table 3. Rate Constants for Exchange of the First α-Proton of Glycine in the Presence of 3 and HFIP Buffers in D_2O [a]

base	f_B[c]	pD	[aldehyde] / M	$f_{\text{3-IM-D}}$[d]	k_o /s^{-1}[e]	k_w /s^{-1}[f]	$(k_{\text{buf}})_{\text{obsd}}$/ M^{-1} s^{-1}[g]	k_B /M^{-1} s^{-1}[h]
HFIP	0.8	10.53	6.0×10^{-3}	0.15	1.7×10^{-6}	1.1×10^{-5}	3.1×10^{-6}	2.6×10^{-5}
		10.52	2.0×10^{-2}	0.39	4.4×10^{-6}	1.1×10^{-5}	8.8×10^{-6}	2.8×10^{-5}
p$K_{BD} = 9.9$[b]								
	0.5	9.80	1.0×10^{-2}	0.32	6.9×10^{-7}	2.2×10^{-6}	4.2×10^{-6}	2.6×10^{-5}
		9.86	5.2×10^{-2}	0.73	1.8×10^{-6}	2.5×10^{-6}	1.2×10^{-5}	3.3×10^{-5}
	0.2	9.35	2.0×10^{-2}	0.45	3.5×10^{-7}	7.8×10^{-7}	2.9×10^{-6}	3.2×10^{-5}

[a] At 25 °C and $I = 1.0$ (KCl). [b] Apparent pK_a of the conjugate acid in D_2O at 25 °C and $I = 1.0$ (KCl). [c] Fraction of the buffer present in the basic form. [d] Fraction of glycine present as the reactive iminium ion 3-IM-D at the given concentration of 3, determined by ^1H NMR analysis of an equilibrium mixture of glycine and the imine. [e] The intercept of plots of k_{ex} against [buffer]$_T$ (Figure 5). [f] Apparent first-order rate constants for solvent-catalyzed deprotonation of 3-IM-D, calculated from the values of k_o as described in the text. [g] The slope of plots of k_{ex} against [buffer]$_T$ (Figure 5). [h] Second-order rate constants for HFIP base-catalyzed deprotonation of 3-IM-D, calculated from the values of $(k_{\text{buf}})_{\text{obsd}}$ as described in the text.

3178

dx.doi.org/10.1021/ja110795m |*J. Am. Chem. Soc.* 2011, 133, 3173–3183

Table 4. Equilibrium Constants in D$_2$O for Addition of Glycine to Carbonyl Compounds, and Second-Order Rate Constants k_{DO} for Carbon Deprotonation of the Imine or Iminium Ion Adduct.[a]
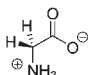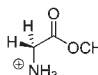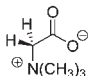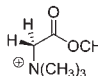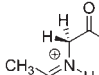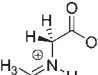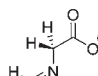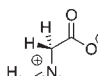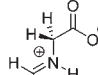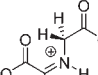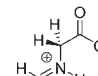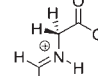
Aldehyde	Carbon Acid	K_{add}[b] (M^{-1})	$(K_{add})^{+}$[c] (M^{-1})	k_{DO}[d] (M^{-1} s^{-1})
		3.5×10^{-2}	5.6×10^{-3}	4.2
		44[e]	0.0033[e]	2.90×10^{-4}
		1.76[e]	72[e]	0.19

[a] At 25 °C and I = 1.0 (KCl). [b] Equilibrium constant for addition of the basic amino form of glycine to the carbonyl compound. [c] Equilibrium constant for addition of glycine zwitterion to the carbonyl compound. [d] Second-order rate constant for carbon deprotonation of the iminium ion adduct by deuterioxide ion in D$_2$O. [e] Data from ref 36.

Table 5. Rate and Equilibrium Constants for Carbon Deprotonation of Glycine and Glycine Derivatives in Water at 25 °C and I = 1.0 (KCl)

Carbon Acid	k_{HO}[a] (M^{-1} s^{-1})	pK_a[b]	Carbon Acid	k_{HO}[a] (M^{-1} s^{-1})	pK_a[b]
	4.5×10^{-5}[c]	28.9[c]		4.1[c]	21.0[c]
	3.3×10^{-4}[c]	27.3[c]		390[c]	18.0[c]
	2.9	21.9		9.0×10^{3}[d]	14[d]
	2.0×10^{-4}	27		ca. 1	ca. 23
	0.13	25		1.1×10^{4}[d]	14[d]
	not determined	ca. 23[e]		7.5×10^{2}[f]	17[f]

[a] Second-order rate constant for deprotonation of the carbon acid by hydroxide ion calculated from data reported in this work, unless noted otherwise. [b] pK_a for ionization of the carbon acid in water calculated from data reported in this work, unless noted otherwise. [c] Data from ref 2. [d] Data from ref 28. [e] Estimated as described in the text. [f] Data from ref 29.

We have estimated k_{HO} for carbon-deprotonation of **2-IMH** by making the assumption that N-protonation of glycine and of **2-IM** will cause similar changes in the thermodynamic and kinetic acidity of the α-amino and α-imino carbon. The α-NH$_3^+$ substituent causes a 4.6-unit decrease in carbon acid pK_a of acetate anion from 33.5 to 28.9 for glycine zwitterion[2,42] and of ethyl acetate from 25.6 to 21.0 for glycine methyl ester.[2,38] By comparison, the α-NH$_2$ substituent is expected to have a small effect on carbon acidity. For example, there is only a 0.5-unit difference between carbon acid pK_a's of 26.5 for acetone and 26.0 for 2-dimethylaminoacetone in DMSO.[45] The weak acidifying effect of an α-dimethylamino group of acetone shows that the inductive effect of this electron-withdrawing group on pK_a is roughly canceled by the opposing enolate destabilization from repulsive interaction between the nonbonding electron lone pair at nitrogen and the delocalized electron pair at the enolate anion.[46] A similar cancellation of inductive and electronic substituent effects has been proposed to explain the small effects of α-hydroxy and α-alkoxy substituents on the kinetic acidity of α-carbonyl carbon.[46−49]

Combining the 4.6-unit effect of the α-NH$_3^+$ substituent on carbon acidity with the ∼0.5-unit effect of the α-NH$_2$ substituent gives a ∼4-unit effect for protonation of the α-amino nitrogen on the carbon acid pK_a of glycine zwitterion and glycine methyl ester (Scheme 4). We assume that protonation of the α-imino nitrogen of **2-IM** will cause a similar 4-unit decrease in the pK_a of the carbon acid, from 27 to 23. The value of k_{HO} = 1 M^{-1} s^{-1} for carbon-acid deprotonation of **2-IMH** reported in Table 5 was calculated from the estimated carbon acid pK_a of 23 using the linear correlation log(k_{HO}/p) = 10.044 − 0.444(pK_a + log p) established in earlier work (Figure 6).[2]

A comparison of kinetic data for deprotonation of **DPL-IMH$_2$** and **3-IMH** by HO$^-$ shows that substitution of the ring 4-CH by −NH$^+$ causes a 6,000-fold increase in k_{HO} for deprotonation of this carbon by hydroxide ion. The linear correlation between log k_{HO} and carbon acid pK_a shown in Figure 6 shows that this change in k_{HO} corresponds to an ∼8-unit decrease in the pK_a of the α-imino carbon. We expect that a large fraction of this 8-unit effect is due to the unit increase in positive charge at the aromatic ring of **DPL-IMH$_2$**. For example, ∼30% (2.1 pK_a units) of the similar 7.8-unit overall effect of the protonated pyridine nitrogen on the acidity constant for the ionization of the carbon acid benzyl phenyl ketone is observed for the charge-conservative nitrogen substitution, and the remaining 70% of this substituent effect (5.7 pK_a units) is expressed when nitrogen is protonated (Chart 3).[50,51] We estimate a pK_a of ∼23 (Table 5) for ionization of **DPL-IMH** by making the assumption that 70% of the total 8-unit effect of the 4-CH for 4-NH$^+$ substitution on carbon acidity is lost upon deprotonation of nitrogen.

4.2. Substituent Effects on the Carbon Acidity of Glycine. *4.2.1. Effect of the α-Iminium Nitrogen.* The addition of
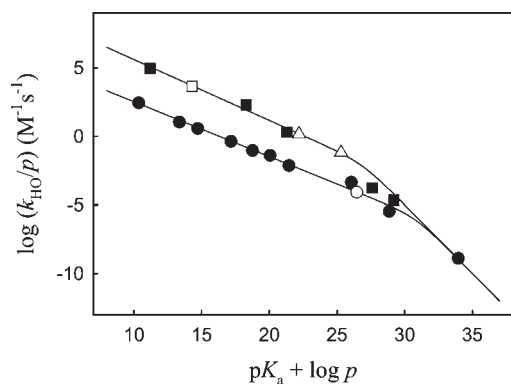
Figure 6. Rate-equilibrium correlations of rate constants, k_{HO} ($M^{-1} s^{-1}$), for deprotonation of α-carbonyl carbon acids by hydroxide ion with the pK_a of the carbon acid. The values of k_{HO} and pK_a were statistically corrected for the number of acidic protons p at the carbon acid. Correlation of $\log(k_{HO}/p)$ for deprotonation of neutral aldehydes, ketones, esters, and acetamide by hydroxide ion, constructed using data from earlier work (●).[38,39,42−44] Excluding the point for acetate anion ($pK_a = 33.5$), the data are correlated by $\log(k_{HO}/p) = 6.496−0.401 (pK_a + \log p)$. Correlation of $\log(k_{HO}/p)$ for deprotonation of cationic ketones and esters (■).[2] The data are correlated by $\log(k_{HO}/p) = 10.044−0.444(pK_a + \log p)$. Data for deprotonation of the acetone-glycine methyl ester iminium ion (□).[27] Data for deprotonation of **1-IM-H** and **3-IM-H** (△). Data for deprotonation of **2-IM** (○).

Scheme 4
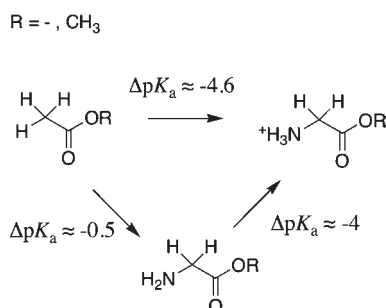
acetone to glycine methyl ester to form the iminium ion results in a 7-unit decrease in the carbon acid pK_a from 21 to 14 (Table 5),[27] while the addition of acetone to the glycine zwitterion results in a similar 7-unit decrease in the carbon acid pK_a from 29 to 22 (Table 5). The overall effect of iminium ion formation on carbon acid pK_a is due to two contributing effects:

(1) The enhancement of intramolecular electrostatic stabilization of the enolate anion by interaction with the cationic nitrogen when the hydrogen-bonded amino protons are replaced by nonpolar organic functionality.[2] This results in a 3-unit larger acidifying effect of the α-NMe_3^+ group at betaine methyl ester ($pK_{CH} = 18.0$) than of the α-NH_3^+ group at glycine methyl ester ($pK_{CH} = 21.0$).[2]

(2) The stabilization of the enolate by direct delocalization of negative charge onto the α-imino carbon (Scheme 2). A similar delocalization of charge is a contributing factor in the ~3-unit lower pK_a of 15.2 for the C-2 proton of 3-cyclohexenone[52] compared with the pK_a of 18.1 for cyclohexanone.[43]

Chart 3
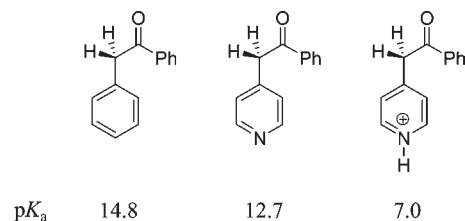
The following two experimental observations suggest that the effect of delocalization of negative charge onto the α-imino carbon on the pK_a of these acetone iminium ions is small.

(1) Oxygen methylation of glycine and betaine zwitterion, which relieves destabilizing electrostatic interactions between neighboring negatively charged oxygen and carbon atoms, causes 8- and 9-unit decreases, respectively, in carbon acid pK_a (Table 5). The observation that oxygen methylation of **1-IMH** causes a similar 8-unit decrease in carbon acid pK_a is consistent with similar destabilizing electrostatic interactions between neighboring negatively charged oxygen and carbon atoms at **1-IMH**, so that there is no detectable relief of this interaction from delocalization of negative charge onto the α-imino carbon of **1-IMH**.

(2) The higher estimated pK_a of 23 for **2-IMH** compared with 22 for **1-IMH** shows that there is no significant stabilization of the glycine enolate of **1-IMH** by the phenyl-for-methyl substitution. If there is little stabilization of **2-IMH** by delocalization of negative charge from the α-imino carbon to the phenyl ring substituent, then the negative charge density at this carbon is almost certainly small.

4.2.2. Effect of Aromatic Substituents at the α-Iminium Nitrogen. Chart 4 summarizes the results of our studies of substituent effect of formation of iminium ions to simple aldehydes R−CHO on the pK_a for deprotonation of the α-amino carbon. The carbon acid pK_a of the iminium ion adduct of glycine to salicylaldehyde (25) is much higher than the pK_a of the iminium ion adduct of glycine to **DPL** (17). Apparently, a very strongly electron-withdrawing group such as the pyridinium ion is required to *drive* the extended delocalization of negative charge onto the α-iminium carbon and cause a further large increase in carbon acidity (Chart 5A). The low carbon acid pK_a of ~18 for the pyridoxamine analogue 4-(aminomethyl)pyridine dication[53] provides supporting evidence that the α-pyridinium substituent provides powerful stabilization of negatively charged carbon.

Table 5 shows that the addition of the strongly resonance electron-withdrawing −CO_2^- substituent to the α-imino carbon of **2-IMH** also drives the extended delocalization of negative charge onto the α-iminium carbon and causes a large decrease in carbon acid pK_a from ~23 to 14[28] for the PG-glycine iminium ion (Chart 5B). We conclude that the second resonance electron-withdrawing group present in the pyruvoyl prosthetic group (−CO_2^-) and PLP (pyridinium cation) provides a large kinetic *push* to electrophilic catalysis of deprotonation of glycine to catalysis of enzymatic reactions that proceed through α-amino carbanion intermediates.

4.3. Relevance to Enzymatic Catalysis. It has been suggested for PLP enzymes that protonation of the pyridine ring of the resonance delocalized α-imino carbanion causes a shift in negative charge density from the α-imino to the α-pyridyl carbon
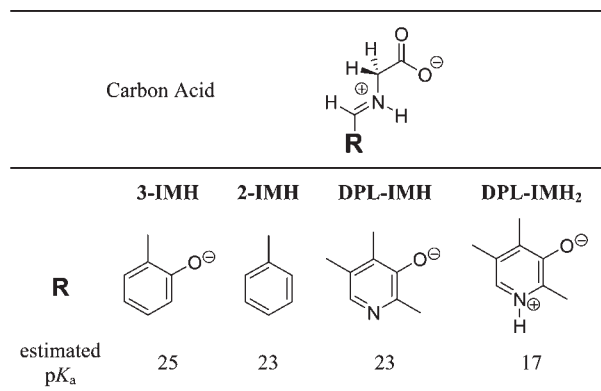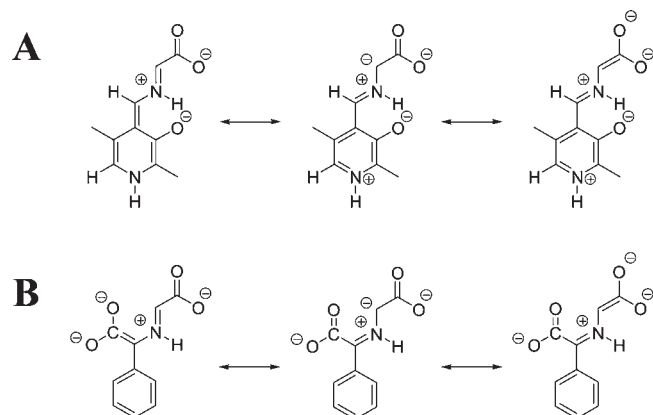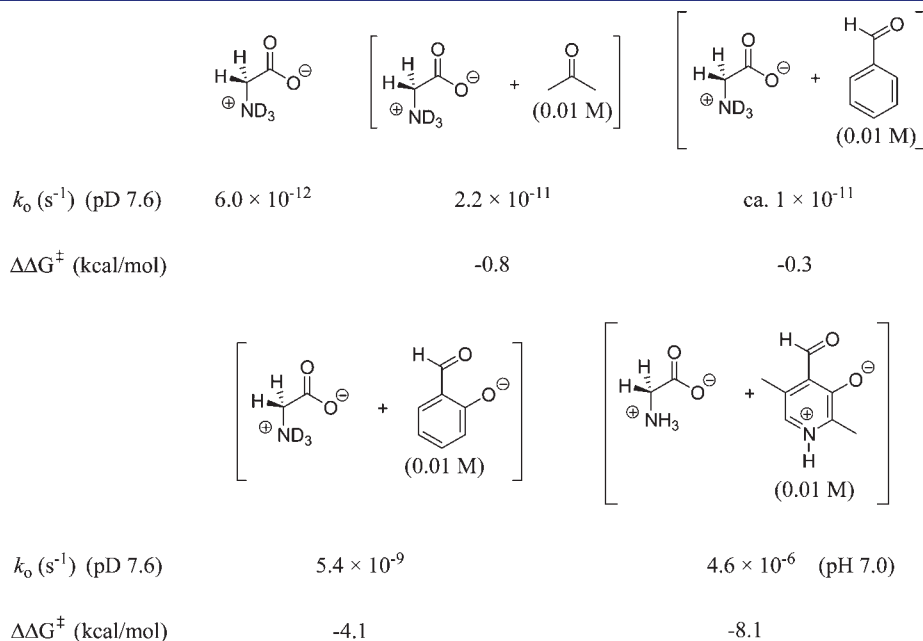
Chart 4

that favors protonation of the α-pyridyl carbon and the 1,3-aza-allylic isomerization reaction that is a step in enzyme-catalyzed transamination reactions.[9] This proposal is consistent with the observation that the PLP cofactor bound to alanine racemase is stabilized by a hydrogen bond to the weakly acidic cation side chain of Arg-219,[54] while the cofactor bound to D-amino acid transaminase[55,56] and alanine glyoxylate aminotransferase[57] is almost certainly protonated by more strongly acidic carboxylic acid side chains of Glu-177 and Asp-180, respectively. The 6-unit difference in the carbon acid pK_a's for **DPL-IMH** and **DPL-IMH$_2$** shows that protonation of the pyridine ring causes a substantial increase in the stability of negative charge at the distant α-amino carbon. This provides direct evidence for an increased delocalization of negative charge across the extended π-system that will favor the enyzme-catalyzed 1,3-aza-allylic isomerization reaction. In summary, PLP-dependent racemases sacrifice part of the cofactor's intrinsic catalytic power by using the cofactor in the neutral pyridine form. Apparently, the mechanistic imperative to direct the reaction toward proton transfer at the α-amino carbon and avoid the wasteful dead-end transamination reaction overrides the competing imperative to utilize the cofactor in its most active form. This shows that the latent catalytic power of PLP-dependent racemases is so great that a portion may be sacrificed to ensure the proper reaction specificity.

4.4. Anatomy of the Rate Acceleration of PLP-Catalyzed Deprotonation of Glycine. Chart 6 compares the first-order rate constants k_o (s^{-1}) for solvent-catalyzed deprotonation of glycine at neutral pL in the absence and presence of 0.01 M carbonyl electrophiles.[58] These data allow a dissection of the contribution of component pieces of the PLP analogue **DPL** to the enormous observed rate acceleration for deprotonation of glycine.

(1) The rate constant $k_o = 2 \times 10^{-11}$ s^{-1} for the reaction in the presence of 0.01 M acetone provides a metric for the intrinsic reactivity of the electrophilic carbonyl group as a catalyst of deprotonation of glycine.

(2) The rate constant of $k_o = 1 \times 10^{-11}$ s^{-1} for the reaction in the presence of 0.01 M benzaldehyde shows that the phenyl for alkyl substitution does not greatly enhance the catalytic reactivity of the carbonyl group.

Chart 5

Chart 6

k_o (s^{-1}) (pD 7.6)	6.0×10^{-12}	2.2×10^{-11}	ca. 1×10^{-11}
$\Delta\Delta G^{\ddagger}$ (kcal/mol)		-0.8	-0.3

k_o (s^{-1}) (pD 7.6)	5.4×10^{-9}	4.6×10^{-6} (pH 7.0)
$\Delta\Delta G^{\ddagger}$ (kcal/mol)	-4.1	-8.1

(3) A comparison of $k_o = 1 \times 10^{-11}$ and $k_o = 5.4 \times 10^{-9}$ s^{-1} for catalysis by 0.01 M benzaldehyde and salicylaldehyde, respectively, shows that the *ortho*-phenoxy substituent stabilizes the transition state for deprotonation of glycine by 3.8 kcal/mol (Chart 6). This is due to the stabilizing intramolecular hydrogen bond between the ring oxygen anion and the iminum ion.[36] The strong intramolecular hydrogen bond causes the carbon acid pK_a to increase from 23 for **2-IMH** to 25 for **3-IMH**. This decrease in carbon acidity attenuates the transition-state stabilization from hydrogen bonding, by causing a decrease in the reactivity of **3-IMH** toward deprotonation by hydroxide ion.

(4) The substitution of the strongly electron-withdrawing pyridinium cation for the phenyl ring at **3-IMH** causes k_o to increase from 5.4×10^{-9} to $\sim 4.6 \times 10^{-6}$ s^{-1}. Neglecting the small effect of the *o*-methyl group on the reactivity of **DPL-IMH$_2$**, there is an additional 4 kcal/mol stabilization of the transition state for deprotonation of glycine (Chart 6). This reflects the strong electron demand of the pyridinium cation, which drives the stabilizing delocalization of charge across the extended π-system.

In conclusion, these results provide an impressive example of how the summation of several relatively small effects in the assembly of the complex molecules **PLP** and **DPL** has produced a type of catalyst of truly extraordinary power.[33] It is an open question whether modern chemists will be able to match the brute-force success of the trial and error of evolution and succeed in designing either small- or large-molecule catalysts with the power of those observed in nature.

■ ASSOCIATED CONTENT

ⓢ Supporting Information. Table S1 of first-order rate constants, k_{ex}, for exchange for deuterium of the first α-proton of glycine in the presence of acetone and HFIP buffers; Table S2 of first-order rate constants, k_{ex}, for exchange for deuterium of the first α-proton of glycine in the presence of benzaldehyde; Table S3 of first-order rate constants, k_{ex}, for exchange for deuterium of the first α-proton of glycine in the presence of salicylaldehyde and HFIP buffers. This material is available free of charge via the Internet at http://pubs.acs.org.

■ AUTHOR INFORMATION

Corresponding Author

anamaria.rios@usc.es; jrichard@buffalo.edu

■ ACKNOWLEDGMENT

■ REFERENCES

(1) Rios, A.; Richard, J. P. *J. Am. Chem. Soc.* **1997**, *119*, 8375–8376.
(2) Rios, A.; Amyes, T. L.; Richard, J. P. *J. Am. Chem. Soc.* **2000**, *122*, 9373–9385.
(3) Rios, A.; Richard, J. P.; Amyes, T. L. *J. Am. Chem. Soc.* **2002**, *124*, 8251–8259.
(4) Richard, J. P.; Amyes, T. L. *Bioorg. Chem.* **2004**, *32*, 354–366.
(5) John, R. A. *Biochim. Biophys. Acta* **1995**, *1248*, 81–96.
(6) Jansonius, J. N. *Curr. Opin. Struct. Biol.* **1998**, *8*, 759–769.
(7) Christen, P.; Mehta, P. K. *Chem. Rec.* **2001**, *1*, 436–447.
(8) Eliot, A. C.; Kirsch, J. F. *Annu. Rev. Biochem.* **2004**, *73*, 383–415.
(9) Toney, M. D. *Arch. Biochem. Biophys.* **2005**, *433*, 279–287.
(10) Sun, S.; Toney, M. D. *Biochemistry* **1999**, *38*, 4058–65.
(11) Watanabe, A.; Yoshimura, T.; Mikami, B.; Hayashi, H.; Kagamiyama, H.; Esak, N. *J. Biol. Chem.* **2002**, *277*, 19166–19172.
(12) Major, D. T.; Gao, J. *J. Am. Chem. Soc.* **2006**, *128*, 16345–16357.
(13) Zhou, X.; Toney, M. D. *Biochemistry* **1999**, *38*, 311–320.
(14) Zhou, X.; Jin, X.; Medhekar, R.; Chen, X.; Dieckmann, T.; Toney, M. D. *Biochemistry* **2001**, *40*, 1367–1377.
(15) Jackson, L. K.; Brooks, H. B.; Osterman, A. L.; Goldsmith, E. J.; Phillips, M. A. *Biochemistry* **2000**, *39*, 11247–11257.
(16) Jackson, L. K.; Brooks, H. B.; Myers, D. P.; Phillips, M. A. *Biochemistry* **2003**, *42*, 2933–2940.
(17) Fogle, E. J.; Liu, W.; Woon, S.-T.; Keller, J. W.; Toney, M. D. *Biochemistry* **2005**, *44*, 16392–16404.
(18) Lin, Y.-L.; Gao, J. *Biochemistry* **2010**, *49*, 84–94.
(19) Kirsch, J. F.; Eichele, G.; Ford, G. C.; Vincent, M. G.; Jansonius, J. N.; Gehring, H.; Christen, P. *J. Mol. Biol.* **1984**, *174*, 497–525.
(20) Hayashi, H.; Kagamiyama, H. *Biochemistry* **1997**, *36*, 13558–13569.
(21) Hayashi, H.; Mizuguchi, H.; Miyahara, I.; Islam, M. M.; Ikushiro, H.; Nakajima, Y.; Hirotsu, K.; Kagamiyama, H. *Biochim. Biophys. Acta* **2003**, *1647*, 103–109.
(22) Liu, W.; Peterson, P. E.; Langston, J. A.; Jin, X.; Zhou, X.; Fisher, A. J.; Toney, M. D. *Biochemistry* **2005**, *44*, 2982–2992.
(23) Miles, E. W. *Chem. Rec.* **2001**, *1*, 140–151.
(24) Dunn, M. F.; Niks, D.; Ngo, H.; Barends, T. R. M.; Schlichting, I. *Trends Biochem. Sci.* **2008**, *33*, 254–264.
(25) Schirch, V.; Szebenyi, D. M. E. *Curr. Opin. Chem. Biol.* **2005**, *9*, 482–487.
(26) Paiardini, A.; Contestabile, R.; D'Aguanno, S.; Pascarella, S.; Bossa, F. *Biochim. Biophys. Acta* **2003**, *1647*, 214–219.
(27) Rios, A.; Crugeiras, J.; Amyes, T. L.; Richard, J. P. *J. Am. Chem. Soc.* **2001**, *123*, 7949–7950.
(28) Crugeiras, J.; Rios, A.; Riveiros, E.; Amyes, T. L.; Richard, J. P. *J. Am. Chem. Soc.* **2008**, *130*, 2041–2050.
(29) Toth, K.; Richard, J. P. *J. Am. Chem. Soc.* **2007**, *129*, 3013–3021.
(30) Jencks, W. P. *Catalysis in Chemistry and Enzymology*, 2nd ed.; Dover: New York, 1987.
(31) Felten, A. E.; Zhu, G.; Aron, Z. D. *Org. Lett.* **2010**, *12*, 1916–1919.
(32) Denesyuk, A. I.; Denessiouk, K. A.; Korpela, T.; Johnson, M. S. *J. Mol. Biol.* **2002**, *316*, 155–172.
(33) Richard, J. P.; Amyes, T. L.; Crugeiras, J.; Rios, A. *Curr. Opin. Chem. Biol.* **2009**, *13*, 1–9.
(34) Morrow, J. R.; Amyes, T. L.; Richard, J. P. *Acc. Chem. Res.* **2008**, *41*, 539–548.
(35) Bordwell, F. G.; Fried, H. E. *J. Org. Chem.* **1981**, *46*, 4327–4331.
(36) Crugeiras, J.; Rios, A.; Riveiros, E.; Richard, J. P. *J. Am. Chem. Soc.* **2009**, *131*, 15815–15824.
(37) Glasoe, P. K.; Long, F. A. *J. Phys. Chem.* **1960**, *64*, 188–190.
(38) Amyes, T. L.; Richard, J. P. *J. Am. Chem. Soc.* **1996**, *118*, 3129–3141.
(39) Amyes, T. L.; Richard, J. P. *J. Am. Chem. Soc.* **1992**, *114*, 10297–10302.
(40) Derived by assuming that the concentration of imine/iminium ion is negligible because only 1% of glycine is converted to the imine/iminium ion adduct in the presence of 0.5 M acetone at pD 10.5.
(41) The secondary solvent deuterium isotope effect for deprotonation of **1-IM-L**, **3-IM-L**, and **2-IM** by lyoxide ion is assumed to be the same as that for deprotonation of acetone: Pocker, Y. *Chem. Ind.* **1959**, 1383–1384.
(42) Richard, J. P.; Williams, G.; O'Donoghue, A. C.; Amyes, T. L. *J. Am. Chem. Soc.* **2002**, *124*, 2957–2968.

3182

dx.doi.org/10.1021/ja110795m |*J. Am. Chem. Soc.* 2011, 133, 3173–3183

(43) Keeffe, J. R.; Kresge, A. J. In *The Chemistry of Enols*; Rappoport, Z., Ed.; John Wiley and Sons: Chichester, 1990; pp 399−480.

(44) Chiang, Y.; Griesbeck, A. G.; Heckroth, H.; Hellrung, B.; Kresge, A. J.; Meng, Q.; O'Donoghue, A. C.; Richard, J. P.; Wirz, J. *J. Am. Chem. Soc.* **2001**, *123*, 8979–8984.

(45) Bordwell, F. G.; Gallagher, T.; Zhang, X. *J. Am. Chem. Soc.* **1991**, *113*, 3495–3497.

(46) Hine, J. *Structural Effects on Equilibria in Organic Chemistry*; Wiley: New York, 1975.

(47) Hine, J.; Hampton, K. G.; Menon, B. C. *J. Am. Chem. Soc.* **1967**, *89*, 2664–2668.

(48) Hine, J.; Mahone, L. G.; Liotta, C. L. *J. Am. Chem. Soc.* **1967**, *89*, 5911–5920.

(49) Crugeiras, J.; Richard, J. P. *J. Am. Chem. Soc.* **2004**, *126*, 5164–5173.

(50) Carey, A. R. E.; Eustace, S.; More O'Ferrall, R. A.; Murray, B. A. *J. Chem. Soc., Perkin Trans. 2* **1993**, 2285–2296.

(51) Carey, A. R. E.; More O'Ferrall, R. A.; Murray, B. A. *J. Chem. Soc., Perkin Trans. 2* **1993**, 2297–2302.

(52) Dzingeleski, G. D.; Blotny, G.; Pollack, R. M. *J. Org. Chem.* **1990**, *55*, 1019–1023.

(53) Crugeiras, J.; Rios, A.; Amyes, T. L.; Richard, J. P. *Org. Biomol. Chem.* **2005**, *3*, 2145–2149.

(54) Shaw, J. P.; Petsko, G. A.; Ringe, D. *Biochemistry* **1997**, *36*, 1329–1342.

(55) Sugio, S.; Petsko, G. A.; Manning, J. M.; Soda, K.; Ringe, D. *Biochemistry* **1995**, *34*, 9661–9669.

(56) Van Ophem, P. W.; Peisach, D.; Erickson, S. D.; Soda, K.; Ringe, D.; Manning, J. M. *Biochemistry* **1999**, *38*, 1323–1331.

(57) Han, Q.; Robinson, H.; Gao, Y. G.; Vogelaar, N.; Wilson, S. R.; Rizzi, M.; Li, J. *J. Biol. Chem.* **2006**, *281*, 37175–37182.

(58) The first-order rate constants k_o (s^{-1}) given in Chart 6 for solvent-catalyzed deprotonation of glycine at neutral pL in the presence of salicylaldehyde and DPL were calculated as $k_o = (k_{LO})_{X-IM}[LO^-]f_{X-IM}$, where $(k_{LO})_{X-IM}$ is the second-order rate constant for deprotonation by lyoxide ion of the corresponding iminium ion (**3-IMH** or **DPL-IMH$_2$**) and f_{X-IM} is the fraction of amino acid that is converted to the iminium ion at the given pL in the presence of 0.01 M salicylaldehyde monoanion and 0.01 M DPL zwitterion, respectively.